Understanding hydrogen plasma processes based on the diagnostic results of 2.45 GHz ECRIS at Peking University*

Wen-Bin Wu(武文斌)[1], Hai-Tao Ren(任海涛)[1,†], Shi-Xiang Peng(彭士香)[1], Yuan Xu(徐源)[1], Jia-Mei Wen(温佳美)[1], Jiang Sun(孙江)[1], Ai-Lin Zhang(张艾霖)[1,2] Tao Zhang(张滔)[1], Jing-Feng Zhang(张景丰)[1], and Jia-Er Chen(陈佳洱)[1,2]

[1] *SKLNPTT&IHIP, School of Physics, Peking University, Beijing* 100871, *China*
[2] *University of Chinese Academy of Sciences, Beijing* 100049, *China*

(Received 24 February 2017; revised manuscript received 19 May 2017; published online 18 July 2017)

Optical emission spectroscopy (OES), as a simple *in situ* method without disturbing the plasma, has been performed for the plasma diagnosis of a 2.45 GHz permanent magnet electron cyclotron resonance (PMECR) ion source at Peking University (PKU). A spectrum measurement platform has been set up with the quartz-chamber electron cyclotron resonance (ECR) ion source [Patent Number: ZL 201110026605.4] and experiments were carried out recently. The electron temperature and electron density inside the ECR plasma chamber have been measured with the method of line intensity ratio of noble gas. Hydrogen plasma processes inside the discharge chamber are discussed based on the diagnostic results. What is more, the superiority of the method of line intensity ratio of noble gas is indicated with a comparison to line intensity ratio of hydrogen. Details will be presented in this paper.

Keywords: electron cyclotron resonance (ECR) ion source, hydrogen plasma, plasma diagnosis, optical emission spectroscopy

PACS: 52.50.Sw, 52.50.Dg, 52.70.–m, 52.70.Kz **DOI:** 10.1088/1674-1056/26/9/095204

1. Introduction

The 2.45 GHz electron cyclotron resonance (ECR) ion source has been widely used in many plasma processing applications and particle accelerators since its invention 30 years ago because of its advantages of high current density, compact structure, long lifetime, and high reliability. In the 1980s, Peking University (PKU) began to carry out relevant research on 2.45 GHz high current ECR ion source.[1] Since then, several 2.45 GHz ECR ion sources have been developed for different applications.[2–5] Although they have been widely used and exhibited excellent performance, the physical processes and plasma characteristics inside the ECR plasma chamber are still not very clear because of the difficulties on the comprehensive studies of the ion source plasma. Fortunately, the study of the behavior of the electrons is helpful to understand the internal plasma mechanisms. For example, the reaction rate coefficient taking into account the energy dependent cross sections is affected by the electron temperature. The plasma density, which usually means the electron density for plasma containing multiply charged ions, is an important parameter. Therefore, it is significant for us to obtain the information of electrons inside the discharge chamber.

There are several methods to make measurements on plasma, such as Langmuir probe, Thomson scattering and optical emission spectroscopy (OES). The Langmuir probe is a common method to diagnose ECR plasma by immersion into the plasma. This probe will then affect the plasma, so we cannot obtain the actual information inside the discharge chamber. In addition, the strong RF power and magnetic field are sometimes limitations for the Langmuir probe.[6] Thomson scattering is usually used as a diagnostic method for the high-temperature and high-density plasma and is developed to use for the ECR plasma. But the Brewster window and baffles as necessary parts for Thomson scattering measurements should be taken into account in the design of the ECR ion source.[7,8] Compared with the above methods, OES has its unique advantages. First, it is a non-invasive technique which measures the line radiation in the visible spectral range. Second, the experimental set-up is very simple. Third, it is a passive and very convenient method which can provide a variety of plasma parameters. However, to achieve the OES measurements, an ECR ion source with special construction and a simplified model for the spectroscopic data analysis are very necessary. At PKU, a specially designed 2.45 GHz PMECR ion source with a quartz chamber has been developed with a patent (Patent Number: ZL 201110026605.4). There are also several ECR ion sources operating with quartz plasma chambers in other laboratories.[9–11] The plasma diagnostic measurements inside our quartz chamber ion source may provide some references to these ion sources. In our previous work, the spectrum measurement platform was set up and relevant experiments were performed using this quartz-chamber ECR ion source. The collisional radiative (CR) model was selected to

*Project supported by the National Natural Science Foundation of China (Grant Nos. 11175009 and 11575013).
†Corresponding author. E-mail: htren@pku.edu.cn
© 2017 Chinese Physical Society and IOP Publishing Ltd

solve the complex problem on spectroscopic data analysis. As presented in Ref. [12], the electron temperature under different gas pressure and magnitude of electron density was measured. However, the dependencies of the electron temperature and electron density on the pressure and the input RF power have not been studied systematically. More relevant experiments are required to comprehend the plasma characteristics inside the plasma chamber, which are presented in this paper.

This paper is organized as follows. The diagnostic methods including the CR model, the methods of line intensity ratio of noble gas and line intensity ratio of hydrogen are described in Section 2. The experimental arrangements are displayed in Section 3. The results and discussion on the electron temperature, electron density, and hydrogen plasma processes are presented in Section 4. At the end of this paper, a conclusion and prospect are presented.

2. Diagnostic method

2.1. Line intensity ratio of noble gas

For low-pressure and low-temperature plasma inside the 2.45 GHz ECR ion source, the CR model which balances the collisional and radiative processes is used. More details of the model have been given in Ref. [13] and we only give a brief introduction here. The population density of state p called $n(p)$ is given by

$$n(p) = R_{\mathrm{n}}(p)\, n_{\mathrm{n}} n_{\mathrm{e}} + R_{\mathrm{i}}(p)\, n_{\mathrm{i}} n_{\mathrm{e}}, \tag{1}$$

where $R_{\mathrm{n}}(p)$ and $R_{\mathrm{i}}(p)$ are the collisional-radiative coupling coefficients describing the ground state and the ionic population process, respectively.

In a spectral measurement, the line intensity I_{pk} is given by

$$I_{pk} = n(p) A_{pk}, \tag{2}$$

where A_{pk} is the transition probability from level p to level k. The line intensity we measured only depends on the population density of state p.

Combining formulas (1) and (2), we can obtain the correlation between the results of the CR model and the measured line intensity as follows:

$$I_{pk} = n_{\mathrm{n}} n_{\mathrm{e}} X_{pk}^{\mathrm{eff}}(T_{\mathrm{e}}, n_{\mathrm{e}}, \ldots),$$

with

$$X_{pk}^{\mathrm{eff}} = (R_{\mathrm{n}}(p) + R_{\mathrm{i}}(p)\, n_{\mathrm{i}}/n_{\mathrm{n}}) A_{pk}. \tag{3}$$

The effective emission rate coefficient X_{pk}^{eff} is the convolution of the cross section for the electron impact excitation process with the Maxwellian electron energy distribution function (EEDF), and is a function of electron temperature T_{e} and electron density n_{e}. The atomic data and analysis structure (ADAS) database provides reliable effective emission rate coefficients of all kinds of elements.

The electron temperature and electron density can be measured by emission spectroscopy using the diagnostic gas on the basis of formula (3). However, an absolutely calibrated system can be easily affected by the density of the particles, the absolute intensity of the line, the detection efficiency of the spectrometer, etc. We can use the line ratio method as below to eliminate these influences:

$$\frac{I_{pk}^{1}}{I_{lm}^{2}} = \frac{n_1}{n_2} \frac{X_{pk}^{\mathrm{eff}}(T_{\mathrm{e}}, n_{\mathrm{e}}, \ldots)}{X_{lm}^{\mathrm{eff}}(T_{\mathrm{e}}, n_{\mathrm{e}}, \ldots)}. \tag{4}$$

In our experiment, He with $E_{\mathrm{th}} \approx 23$ eV and Ar with $E_{\mathrm{th}} \approx 13$ eV are used as auxiliary diagnostic gases for the determination of electron temperature T_{e} and electron density n_{e}. To simplify the calculation, the ratio of particle density is 1:1. The ratio of line intensity can be measured with the spectrometer. Therefore, the ratio of effective emission rate coefficient which depends on T_{e} and n_{e} can be identified. It is noteworthy that the lines we used are the radiation of atomic He and Ar.

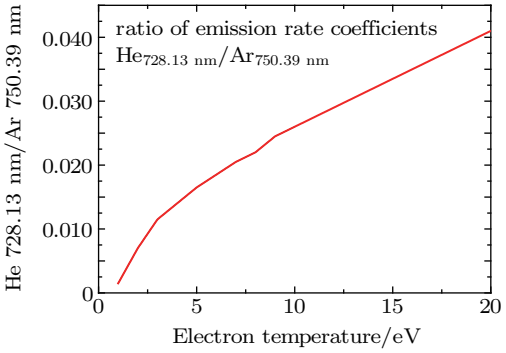


Fig. 1. (color online) The ratio of emission rate coefficients corresponding to He line at 728.13 nm to Ar line at 750.39 nm as a function of the electron temperature.

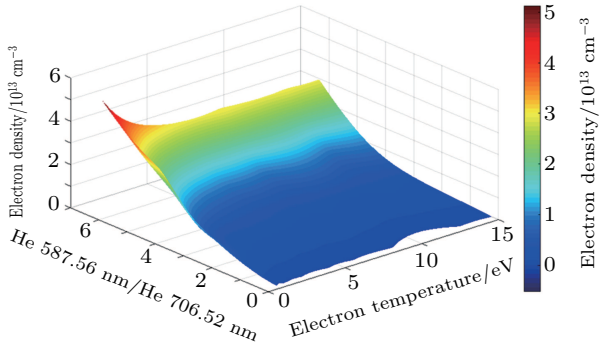


Fig. 2. (color online) The electron density as a function of the electron temperature and ratio of emission rate coefficients for He line at 587.56 nm to 706.52 nm.

Figure 1 shows the ratio of emission rate coefficients corresponding to He line at 728.13 nm to Ar line at 750.39 nm as a function of T_{e}. Relevant research indicates that the ratio is

sensitive to T_e and less sensitive to n_e,[14] therefore T_e can be determined from formula (4) by measuring the ratio of these two line intensities. The line ratio of He line at 587.56 nm to 706.52 nm is sensitive to n_e and it is recommended.[15] Figure 2 shows n_e as a function of T_e and the ratio of emission rate coefficients for the two He lines.

2.2. Line intensity ratio of hydrogen

For plasma on the state of local thermal equilibrium, electron temperature T_e can be determined by the ratio of two line intensities of the same atom.[16] The line intensity ratio can be given as

$$\frac{I_1}{I_2} = \frac{A_1 g_1 \lambda_2}{A_2 g_2 \lambda_1} \exp\left(-\frac{E_1 - E_2}{kT_e}\right). \tag{5}$$

Formula (5) can be written as follows for the evaluation of the electron temperature:

$$T_e = \frac{E_1 - E_2}{\ln\frac{g_1 A_1}{g_2 A_2} - \ln\frac{I_1}{I_2} - \ln\frac{\lambda_1}{\lambda_2}} \quad [\mathrm{eV}], \tag{6}$$

where A, g, I, λ, and E are the transition coefficient, the statistical weight, the emission intensity, the wavelength, and the energy of the upper level of the emission line (in units of eV), respectively. For Balmer series of hydrogen, these constants are precisely available and are recommended for electron temperature diagnosis. Table 1 presents the spectral line data of hydrogen Balmer series.

In our measurements, H_α and H_β are used for the determination of the electron temperature. Figure 3 shows the line intensity ratio of H_α to H_β as a function of T_e.

Table 1. Hydrogen Balmer series spectral line data.

Balmer series	Wavelength/nm	Statistical weight	Transition coefficient/μs^{-1}	Energy/eV
H_α	656.28	18	44.1	12.09
H_β	486.13	32	8.4	12.75
H_γ	434.05	50	2.5	13.05

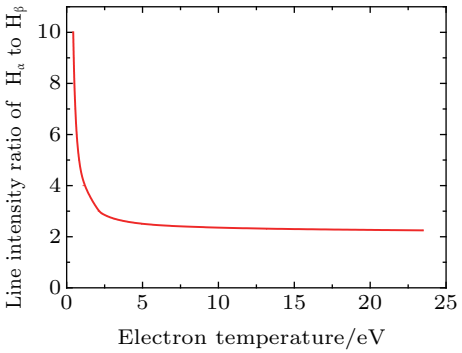


Fig. 3. (color online) The line intensity ratio of H_α to H_β as a function of the electron temperature.

3. Experimental arrangements

Figure 4 is a cut view of the quartz-chamber ECR ion source at PKU. The main parts of the ion source consist of an RF matching section (microwave window), a 90 mm×90 mm quadrate source body, and a three-electrode extraction system. It can produce 84 mA hydrogen ion beam working at pulsed model (10% duty factor) and its rms normalized emittance is smaller than 0.2 π·mm·mrad. The magnetic field of the ion source is provided by three NdFeB rings which are separated by non-magnetic metal gaskets. What deserves to be mentioned is that the discharge chamber is made of high transmissivity quartz, and the plasma spectrum can pass though the quartz and gaps between the magnetic rings. Therefore, plasma diagnosis can be performed for this specially designed ion source. Figure 5 is a schematic illustration of the experimental set-up for plasma diagnosing at PKU. The test platform is composed of the ECR ion source, a gas control system, and a diagnostic system. In order to simplify the calculation of spectrum, mixed He and Ar are used as diagnostic gases from one gas cylinder with He and Ar mixed at the ratio of 1:1. Therefore, a two-channel gas control system with calibrated flow meters is needed to mix the noble gases and hydrogen at specified fractions (He Ar : $H_2 = 1:5$ or 1:10) instead of the three-channel gas control system we used before. With this improvement, the accuracy of the experimental results can be significantly improved for the precise ratio of particle density. The diagnostic system consists of an optic fiber, a high-resolution spectrometer (AvaSpec-USL3648) in the spectral range of 410 nm to 920 nm, and a computer for data analysis.

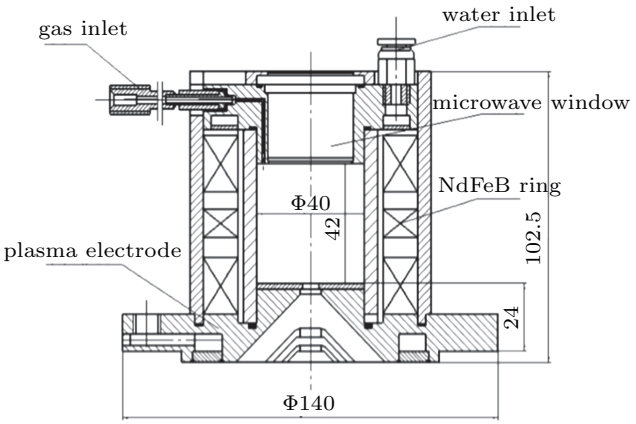


Fig. 4. A cut view of the quartz-chamber ECR ion source at PKU.

4. Results and discussion

This section presents the results of electron temperature T_e and electron density n_e as functions of the gas pressure and the input RF power. What is more, the measurements with different ratios of the mixed noble gases to hydrogen (1:5 or 1:10) are also performed in our research. Finally, a comparison is

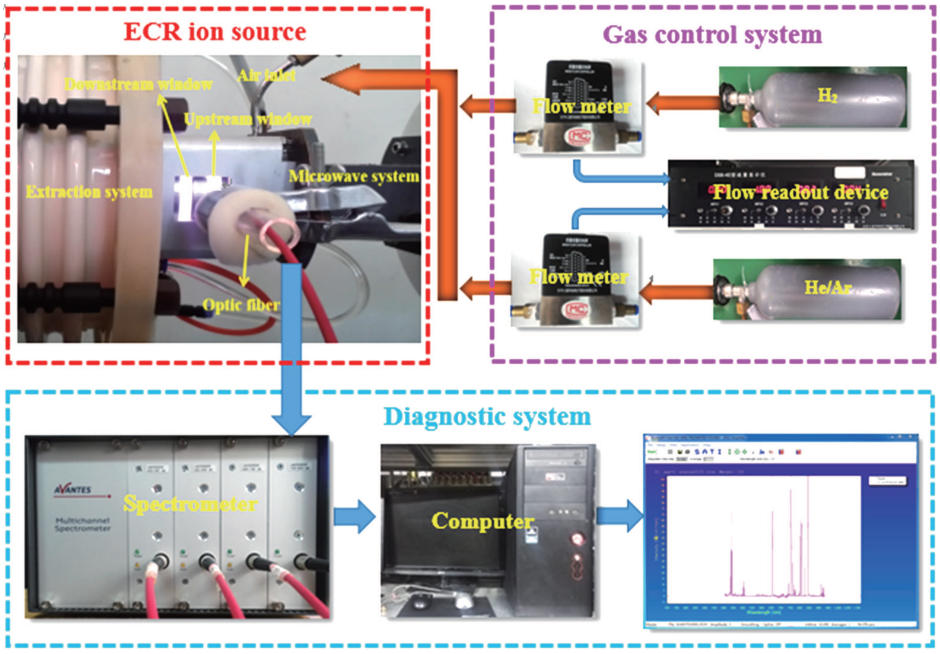


Fig. 5. (color online) Schematic illustration of the experimental set-up.

made between the methods of line intensity ratio of hydrogen and line intensity ratio of noble gas. There are two things that should be kept in mind. Firstly, the gas pressure is the pressure of the vacuum chamber, which does not reflect the actual pressure of the discharge chamber. It should be lower than the pressure of the discharge chamber for the high gas resistance of the extraction system. Secondly, the RF power we mentioned is the peak RF power generated by the microwave generator (10% duty factor). In addition, each plotted point of the results is the average of three separate measurements.

4.1. Electron temperature

Figure 6 shows the dependence of the electron temperature on the gas pressure. We can notice that the electron temperature first decreases significantly and then decreases slowly as the gas pressure increases. This trend is similar to the results reported by others using Thomson scattering measurements and Langmuir probes.[8,17] This phenomenon can be attributed to the change of mean free path of the electrons. The increasing gas pressure means higher collision frequency and more energy loss, thus the electron temperature goes down. This has been confirmed by the achievement of 2.45 GHz PMECR ion source at PKU. It can produce more than 100 mA hydrogen ion beam working at pulsed mode, and more than 20 mA H_3^+ (43.2%) and 40 mA H_2^+ (47.7%) have been obtained with suitable parameters.[18] The cross sections of plasma processes are affected by the electron energy and will have an effect on the composition of the extracted currents. Therefore, the dependence of species fraction on the gas pressure of this ion source is presented for the comprehension of how the electron energy influences the behavior of different ions. As shown in Fig. 7, the fractions of the extracted H_2^+ and H_3^+ beams are sensitive to the gas pressure and have opposite trends, the extracted H_2^+ beam decreases and H_3^+ beam increases as the gas pressure rises. This is understandable by analyzing the hydrogen plasma processes inside the discharge chamber shown in Fig. 8. Firstly, H_2^+ ions inside plasma are created by direct ionization of H_2, the cross section of H_2 direct ionization firstly increases as the energy increases then decreases with an optimal energy of 70 eV. For 2.45 GHz ECR ion source, the electron energy is usually below 20 eV. Therefore, the H_2^+ production cross section will decrease as the pressure rises. Secondly, H_3^+ ions are produced by the dissociative attachment of H_2^+ with a threshold energy of 0 eV. This reaction rate increases as the pressure rises. Therefore, the generation of H_2^+ decreases and the production of H_3^+ increases as the pressure rises for the diminution of the electron energy.

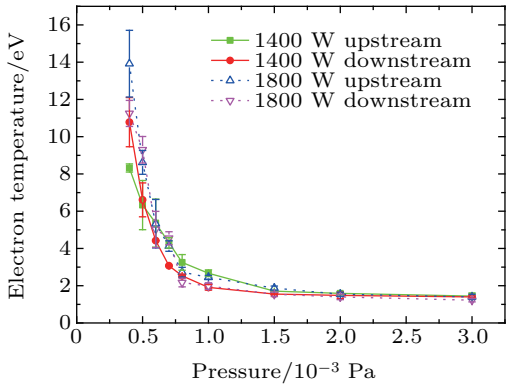


Fig. 6. (color online) Dependence of the electron temperature on the gas pressure.

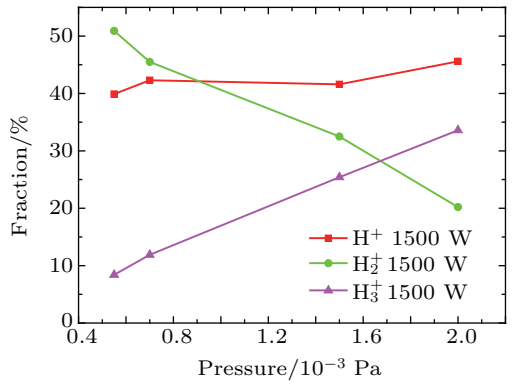


Fig. 7. (color online) Dependence of the extracted species fraction on the gas pressure for hydrogen molecular ion source at PKU.

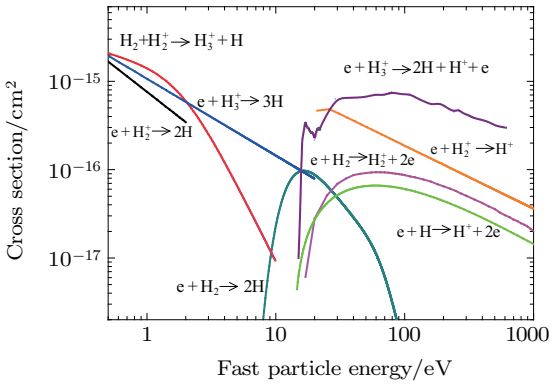


Fig. 8. (color online) Cross sections of some physical process inside the hydrogen ion source.[19]

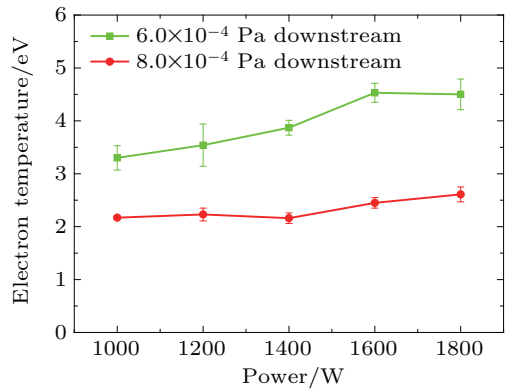


Fig. 9. (color online) Dependence of the electron temperature on the RF power.

In some papers,[8,20] the electron temperature is considered to be nearly constant over the whole RF power range since the electron temperature is primarily influenced by the gas pressure as shown in Fig. 6. This behavior is basically in accordance with our results in Fig. 9 except for a slight growth of electron temperature with increasing RF power. This is also understandable since the electric field amplitude of the propagating wave is proportional to the square root of the RF power. Therefore, the electrons can gain more energy from the electric field and the electron temperature will increase. Our results are reasonable from this point of view.

4.2. Electron density

Figure 10 presents the dependence of the electron density on the gas pressure. The electron density goes up at first, and then decreases as the gas pressure increases. Two probable interpretations are provided for comprehension of this behavior. Firstly, the RF power is sufficient at the beginning, and the electron density increases as the pressure rises because of more ionization of hydrogen molecular. However, the electron density will reach a limitation according to the law of energy conservation for a certain RF power level. In contrast, the higher gas pressure means lower electron energy, which means that the cross section of dissociative recombination of H_2^+ and other process such as recombination of H^+ will increase and more electrons will be consumed during these processes. This could be a reasonable explanation for the trend observed in Fig. 10. Secondly, we can also interpret this trend from Paschen's law. The breakdown voltage is high at both low and high pressures, which means that the formation of the plasma is difficult in these cases. As a consequence, there must be a vertex of electron density as the gas pressure changes. More relevant research is needed for confirming these speculations. Moreover, the maximum in the electron density curves shifts to higher pressure when the input RF power increases. Therefore, it is crucial to match the gas pressure with the input RF power for higher electron density. This phenomenon of the electron density is also confirmed by the experimental results of the high current hydrogen molecular ion source at PKU. As we know, the extracted current is a space-charge-limited current for the ECR ion source, and the current density is proportional to the plasma density inside the discharge chamber. Therefore the intensity of the extracted current can be reflected by the plasma density inside the ECR chamber. Figure 11 shows the extracted current (positive correlation of electron density) as a function of the gas pressure. The behavior is in accordance with the measurements in Fig. 10. What is more, the electron temperature and electron density measured at upstream and downstream are very close as shown in Figs. 6 and 10 because of the similar magnetic field of these two positions.

Not only the gas pressure but also the RF power have an impact on the electron density. It can be noticed in Fig. 12 that the electron density increases rapidly as the RF power increases. This trend is easy to understand, as the RF power rises, a large number of particles are ionized with more electrons generated. It should be pointed out that the increase trend is much more significant than that in Ref. [6] because of more sufficient microwave coupling in our measurement. As shown in Fig. 4, a specially designed alumina dielectric microwave window is used for the microwave coupling between the rectangle waveguide and the plasma chamber. Therefore, the electron density varying with the RF power is in fact a reflection

of microwave coupling efficiency. What is more, the electron density also has an influence on the species fraction of the final extraction beam. For example, H_3^+ has a large dissociative recombination cross section with electrons as shown in Fig. 8, thus low RF power is beneficial to fraction of H_3^+ according to Fig. 12. What is more, a moderate RF power is recommended to the improvement of H_2^+ fraction. Firstly, a low electron density is insufficient since the H_2^+ ions are created by direct ionization of hydrogen molecules with electrons. Secondly, a high electron density will consume the H_2^+ ions since the dissociative recombination of H_2^+ with electron also has a large cross section as shown in Fig. 8. These laws have been proved by the results of cluster ECR ion source at PKU.[18]

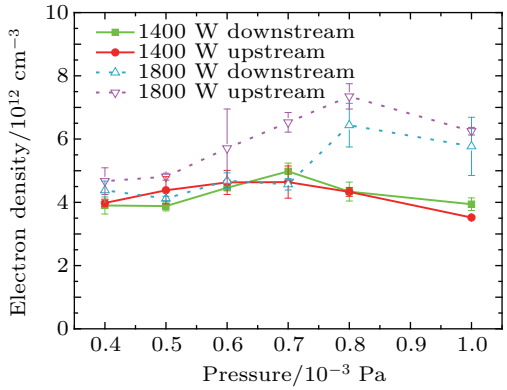


Fig. 10. (color online) Dependence of the electron density on the gas pressure.

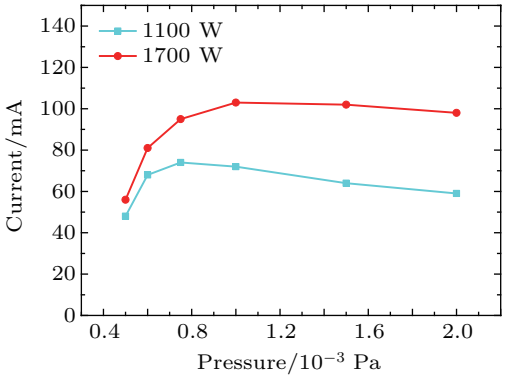


Fig. 11. (color online) The current as a function of the gas pressure for hydrogen molecular ion source at PKU with Φ30 mm discharge chamber.

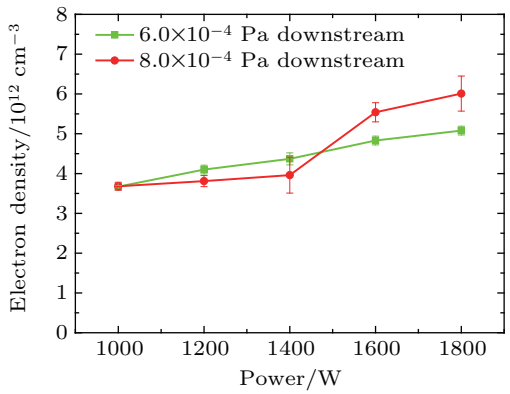


Fig. 12. (color online) Dependence of the electron density on the RF power.

4.3. Proportion of mixed noble gases

Generally speaking, a small percentage of mixed noble gases are added to the discharge chamber just for diagnostic purpose, the results should not be affected a lot by the ratio of the mixed noble gases to hydrogen. However, it can be noticed in Figs. 13 and 14 that the electron temperature decreases and the electron density increases as the proportion of mixed noble gases increases. In other words, the electron temperature we measured is lower and the electron density is higher than the results for pure hydrogen. It seems that the method of line intensity ratio of noble gas will bring some problems. However, this phenomenon is also reasonable for the distinction of ionization energy of different gas. The ionization energy of hydrogen atom is lower than Ar and He in which situation electrons can gain more energy from the RF power. Therefore, the electron temperature of pure hydrogen is higher than the gas mixture. As mentioned in Section 2, the diagnosis of the electron density is based on the electron temperature, the decrease of the electron temperature will lead to the increase of the electron density for a certain line ratio as shown in Fig. 2. What is more, the proportion of the mixed noble gases makes no difference to the trend we observed as shown in Figs. 13 and 14. From this point of view, the method of line intensity ratio of noble gas is still a very powerful tool that we can use for plasma diagnosis.

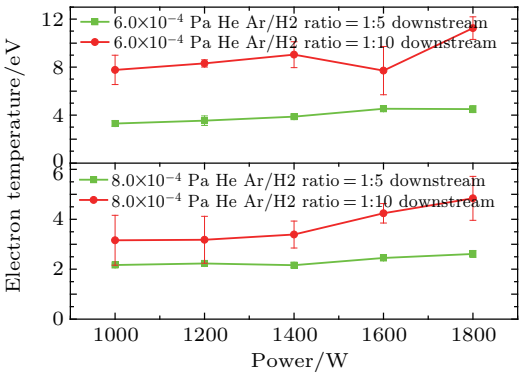


Fig. 13. (color online) Dependence of the electron temperature on the RF power for different ratios of mixed noble gases to hydrogen.

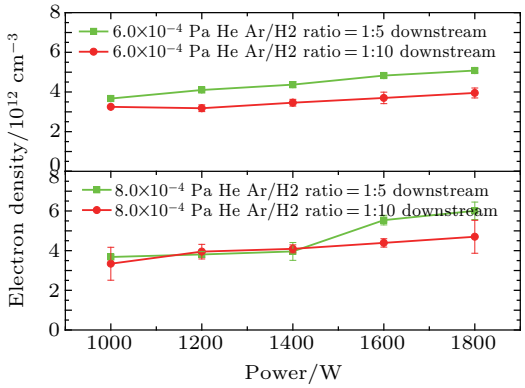


Fig. 14. (color online) Dependence of the electron density on the RF power for different ratios of mixed noble gases to hydrogen.

4.4. Comparison with other methods

Some research indicated that the electron temperature can be determined using the line intensity ratio of hydrogen.[21,22] This method is also used in our work by measuring the line intensities of H_α and H_β for the determination of the electron temperature. Figure 15 presents the results for pure hydrogen and hydrogen with noble gas (gas mixture). It is obvious that the electron temperature is higher for pure hydrogen which is in accordance with the conclusion in Subsection 4.3. As mentioned in Subsection 4.1, the electron temperature first decreases significantly and then decreases slowly as the gas pressure increases. This trend is similar to the results reported by others using Thomson scattering measurements and Langmuir probes. Thus this law should be a typical result and should not be different for different methods. However, the hydrogen method cannot reflect this law as shown in Fig. 16 because this method is based on the assumption of local thermal equilibrium (LTE). For plasma inside ECR ion source, the LTE assumption is not valid. The line intensity ratio of noble gas is without the limitation of LTE assumption and is reliable for electron temperature diagnosis. Based on these facts, more improvements are needed for the use of line intensity ratio of hydrogen inside ECR chamber, and the line intensity ratio of noble gas is recommended. But this does not mean the line intensity ratio of hydrogen is useless. On the contrary, this method can play an important role in the diagnosis for degree of dissociation, etc. More relevant work about hydrogen spectrum will be performed in the future.

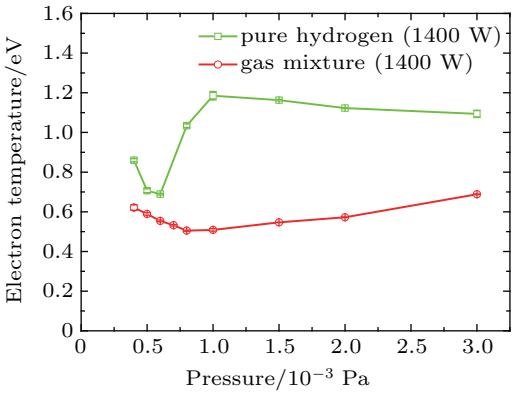


Fig. 15. (color online) Dependence of the electron temperature on the gas pressure obtained by the method of line intensity ratio of hydrogen.

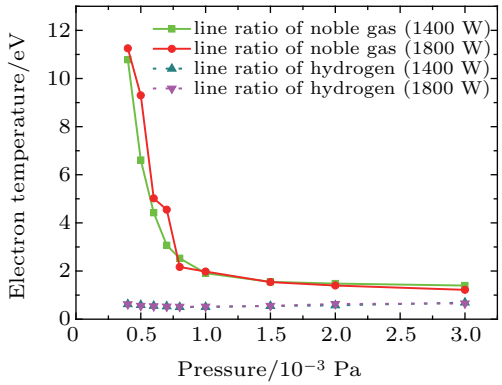


Fig. 16. (color online) Comparison of line intensity ratio of hydrogen and line intensity ratio of noble gas.

5. Conclusion and prospects

The electron temperature and electron density are measured for plasma inside 2.45 GHz ECRIS at PKU with OES method. The results show that the electron temperature decreases significantly as the gas pressure increases and nearly unaffects input RF power. The electron density increases rapidly with increasing RF power. And it is crucial to match the gas pressure with the input RF power for higher electron density. What is more, the species fraction and extraction beam current are mainly determined by the electron energy and electron density, respectively. All of the details and explanations are presented in this paper. In addition, we illustrate the influence of the noble gas on the diagnostic results and show the feasibility of the line intensity ratio method for plasma diagnosis. At last, the superiority of line intensity ratio of noble gas is indicated with a comparison to the line intensity ratio of hydrogen.

A new 2.45 GHz microwave driven H^- ion source with a quart window is designed for plasma diagnosis, more relevant work such as atomic and molecular spectroscopy for hydrogen plasma will be performed in the future.

References

[1] Peng S X, Song Z Z, Yu J X, Ren H T, Zhang M, Yuan Z X, Lu P N, Zhao J, Chen J E, Guo Z Y and Lu Y R 2010 *Proceedings of ECRIS10* August 23–26, 2010, Grenoble, France, p. 102

[2] Song Z Z, Jiang D and Yu J X 1996 *Rev. Sci. Instrum.* **67** 1003

[3] Peng S X, Zhang M, Song Z Z, Xu R, Zhao J, Yuan Z X, Yu J X, Chen J and Guo Z Y 2008 *Rev. Sci. Instrum.* **79** 02B706

[4] Ren H T, Peng S X, Zhang M, Zhou Q F, Song Z Z, Xu Y, Lu P N, Xu R, Zhao J, Yu J X, Lu Y R, Guo Z Y and Chen J E 2010 *Rev. Sci. Instrum.* **81** 02B714

[5] Peng S X, Zhang T, Ren H T, Zhang A L, Xu Y, Zhang J F, Guo Z Y and Chen J E 2016 *Rev. Sci. Instrum.* **87** 02B125

[6] Gobin R, Benmeziane K, Delferrière O, Ferdinand R, Girard A and Harrault 2005 *AIP Conference Proceedings* **763** 289

[7] Sakoda T, Momii S, Uchino K, Muraoka K, Bowden M, Maeda M, Manabe Y, Kitagawa M and Kimura T 1991 *Jpn. J. Appl. Phys.* **30** L1425

[8] Bowden M D, Okamoto T, Kimura F, Muta H, Uchino K, Muraoka K, Sakoda T, Maeda M, Manabe Y, Kitagawa and Kimura T 1993 *J. Appl. Phys.* **73** 2732

[9] Schmitt C, Bowers M, Collon P, Robertson D, Henderson D, Jiang C L, Pardo R C, Rehm E, Scott R, Vondrasek R, Calaprice F, Haas E D and Galbiati C 2008 *Proceedings of ECRIS08*, September 15–18, 2008, Chicago, Illinois, USA, p. 46

[10] Button D and Hotchkis M A C 2008 *Proceedings of ECRIS08*, September 15–18, 2008, Chicago, Illinois, USA, p. 53

[11] Thuillier T 2013 *Proceedings of Cyclotrons2013,* September 16–20, 2013 Vancouver, BC, Canada, p. 130

[12] Xu Y, Peng S X, Ren H T, Zhao J, Chen J, Zhang T, Zhang J F, Guo Z Y and Chen J E 2014 *Proceedings of ECRIS2014* August 24–28, 2014, Nizhny Novgorod, Russia, p. 20

[13] Fantz U 2006 *Plasma Sources Sci. Technol.* **15** S137

[14] Fantz U, Falter H, Franzen P, Wünderlich D, Berger M, Lorenz A, Kraus W, McNeely P, Riedl R and Speth E 2006 *Nuclear. Fusion* **46** S297
[15] Fantz U 2004 *Contrib. Plasma Phys.* **44** 508
[16] Qayyum A, Zeb S, Naveed M A, Ghauri S A, Zakaullah M and Waheed A 2005 *J. Appl. Phys.* **98** 103303
[17] Oomori T, Tuda M, Ootera H and Ono K 1991 *J. Vac. Sci. Technol. A* **9** 722
[18] Xu Y, Peng S X, Ren H T, Zhao J, Chen J, Zhang A L, Zhang T, Guo Z Y and Chen J E 2014 *Rev. Sci. Instrum.* **85** 02A943
[19] Jones E M 1977 *Atomic Collision Processes in Plasma Physics Experiments II*, Report CLM-R 175 UKAEA
[20] Suzuki T, Sawado Y, Lida T and Fujii Y 2004 *Rev. Sci. Instrum.* **75** 1520
[21] Lawrie S R, Faircloth D C and Philippe K 2012 *Rev. Sci. Instrum.* **83** 02A704
[22] Jin D Z, Yang Z H, Tang P Y, Xiao K X and Dai J Y 2009 *Vacuum.* **83** 451